

Mitigating seismic noise with an acoustic blanket—the promise and the challenge

W.S. ROSS, P.J. LEE, S.E. HEINEY, and J.V. YOUNG, ExxonMobil Upstream Research Company, Houston, USA
E.N. DRAKE, ExxonMobil Research and Engineering Company, Clinton, New Jersey, USA
R. TENGHAMN and A. STENZEL, Petroleum Geo-Services, Houston, USA

Waterborne seismic noise is a broad category encompassing well-known noises like marine multiples, seismic interference noise, noise emanating from offshore structures and propagating into the marine environment, and even borehole-trapped noise. For several years, we have been studying the potential of bubble curtains for suppressing these types of noises.

The work began in the area of multiple suppression. Processing approaches to multiple suppression have a long history in the seismic industry, dating back at least to Backus' classic 1959 GEOPHYSICS paper on removal of "singing" from seismic records by deconvolution. Each successive generation of processing methods has improved multiple suppression by relying on more accurate models of the noise-generation mechanisms. However, over the course of more than 30 years of improving processing-only methods, suppressing such noises is still a key issue in seismic data processing, and still a key risk factor in seismic interpretation and attribute analysis. One reason is that geophysical data are applied in contexts that are more demanding from the noise-suppression perspective: The current geologic areas where we are operating are more structurally complex and involve stronger multiple generators (e.g., salt and volcanics) than in earlier years. Another reason for the continued difficulty with multiple suppression is that more is required of data today than in the past. A structural interpretation is only the beginning—now we also require good amplitudes for AVO, attribute analysis, and inversions.

One approach toward improving multiple suppression in today's difficult data areas is to continue to improve our physical description of multiple-generation mechanisms, including extending algorithms into 3D and improving the accuracy of estimating multiple characteristics from the data. A number of new methods have resulted from this approach in recent years, including the surface-related multiple elimination method and several model-based methods. Improving our models will continue to be an important part of the development of multiple-suppression techniques.

However, a processing-only approach has its limits. The level of improvement that each successive generation of methods achieves is smaller and smaller. This methodology may have reached diminishing returns. Multiple suppression by a factor of 3-5 is readily achievable by processing. However, multiples generated from strong subsurface reflectors may be an order of magnitude larger than the primaries of interest (though obviously not larger than the primaries that generated them).

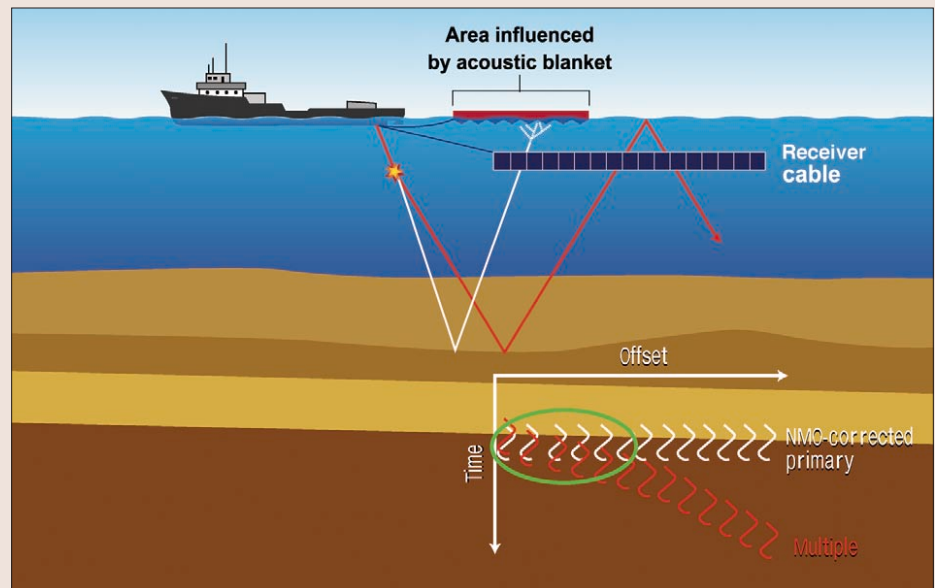


Figure 1. Acoustic blanket concept. The acoustic blanket blocks downgoing waves at any portion of the air-water interface it covers. The white ray path would have been recorded as a multiple on the near offsets, but is intercepted by the acoustic blanket. The red ray path will be recorded on the far offsets, where there is moveout between multiple and primary and, hence, processing methods are effective. The blanket should cover the portion of a CMP gather shown in the green circle, where primary-to-multiple differential moveout is small.

An alternative, the one underlying the methods proposed in this paper, is to attempt multiple suppression in data acquisition. Methods such as OBC and over-under sources/streamers adopt this philosophy by modifying acquisition to improve multiple suppression. Another example is multiazimuth acquisition, in which acquisition is tailored to the requirements of complex multiple generation. The method proposed here attempts to mitigate multiples by blocking their generation at the air-water interface. The air-water interface is the most important horizon in the generation of surface multiples and has been the focus of surface-related processing for several years. We extend this approach to the acquisition realm. We refer to the method of blocking or absorbing acoustic energy from downward reflection at the air-water interface as an "acoustic blanket" (Figure 1).

Early in our work, we studied many potential materials and configurations that could provide absorption or diminution of the downgoing reflection from the air-water interface. Laboratory studies demonstrated more success with methods of deflection than methods of absorption. Even highly attenuative materials represented a large impedance contrast to the acoustic wave, and as such reflected the acoustic wave rather than attenuating it. These results highlighted the value of creating a surface that would be highly reflecting and have an advantageous shape, rather than attempting to absorb the acoustic wave.

Scaling laboratory results to actual field acquisition dimensions highlighted the enormous volumes that would be required for objects to deflect low-frequency acoustic waves. Objects need to be on the order of a Fresnel zone at the air-

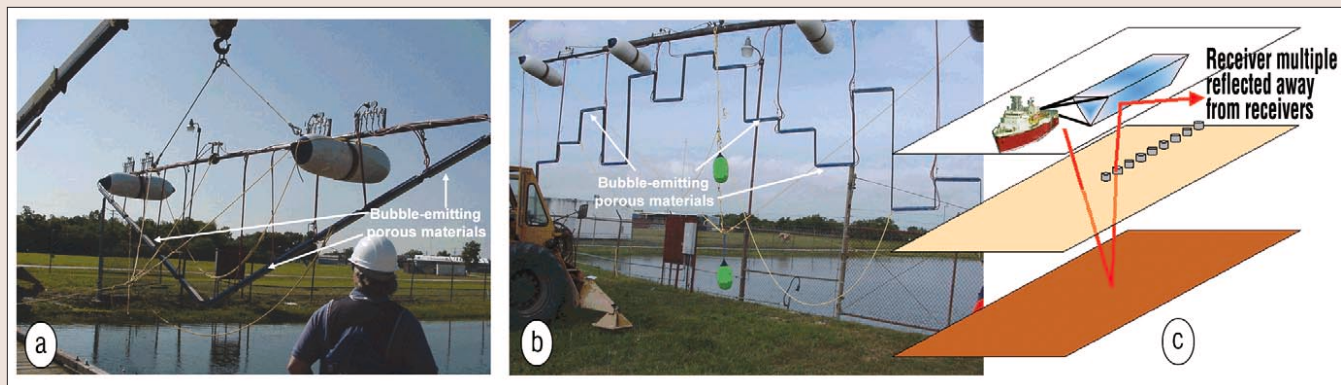


Figure 2. Two concepts for the shape of the bubble curtain in the vertical plane behind the vessel. (a) inverted V; (b) a surface of heights arranged in a pseudorandom pattern; (c) extension of the curtain in the inline direction resulting from the latency of bubbles rising slowly out of the water.

water interface to have an appreciable effect on the reflection process at that interface. It was natural to consider the use of air-bubble curtains in order to create such large objects. More than a decade before our work, Domenico (1982) and Clark (1986) had proposed bubble curtains for this use. More recently, Berhens (1999) also employed bubbles for noise suppression. However, our application, though similar in some respects, had significant differences.

Clark had proposed a curtain designed not for high reflection but for refraction of the acoustic wave. Clark's invention intended the acoustic wave to travel *through* the curtain, and modify its propagation path by the consequent refraction. In our approach (Lee et al., 2003), with the insights developed from laboratory work, the curtain would deflect substantially all the incoming acoustic wave, presenting a barrier of very high reflectivity, ideally as high as 0.9.

Domenico proposed interfaces of very high reflectivity. However, his proposed device was much smaller than ours (and Clark's), with the intended deployment local to the source. The Fresnel zone of the upgoing source wave near the source is much smaller than that of an upcoming wave from deeper horizons like the water bottom and, hence, it was more easily deployed and had a significantly lower air requirement than ours.

Berhens tailored bubble sizes to absorb the acoustic wave. This is a tricky process, which works in certain specialized applications where the noise is sufficiently narrow band to allow the tuning of bubble sizes to noise frequencies of interest. However, this approach is difficult to extend to all applications discussed below.

What resulted from this work, however, is not a single application but an entire range of applications in the suppression of marine noises. Moving to the highly reflective concept made it possible to consider several areas of implementation that benefit our industry.

Overview of applications. In this section, we will briefly review several possible applications. The following section will discuss the multiple suppression application in more detail.

Multiple suppression. In this application, a bubble curtain is deployed at the air-water interface in such a way as to deflect upcoming primary signal. The bubbles are emitted from a plane behind the seismic vessel (or source vessel in OBC acquisition). Figure 2 shows two concepts for the shape of the bubble curtain in that plane. The first (Figure 2a) is an inverted "V," sometimes referred to as a "wedge baffle." Being a highly reflective surface, the lower edge of the V deflects the multiple off to the side in the crossline direction, away from the streamers (or bottom cables in OBC acquisition). The second concept (Figure 2b) is a surface of heights arranged in a pseudorandom pattern. This pattern, based on the concept of "prim-

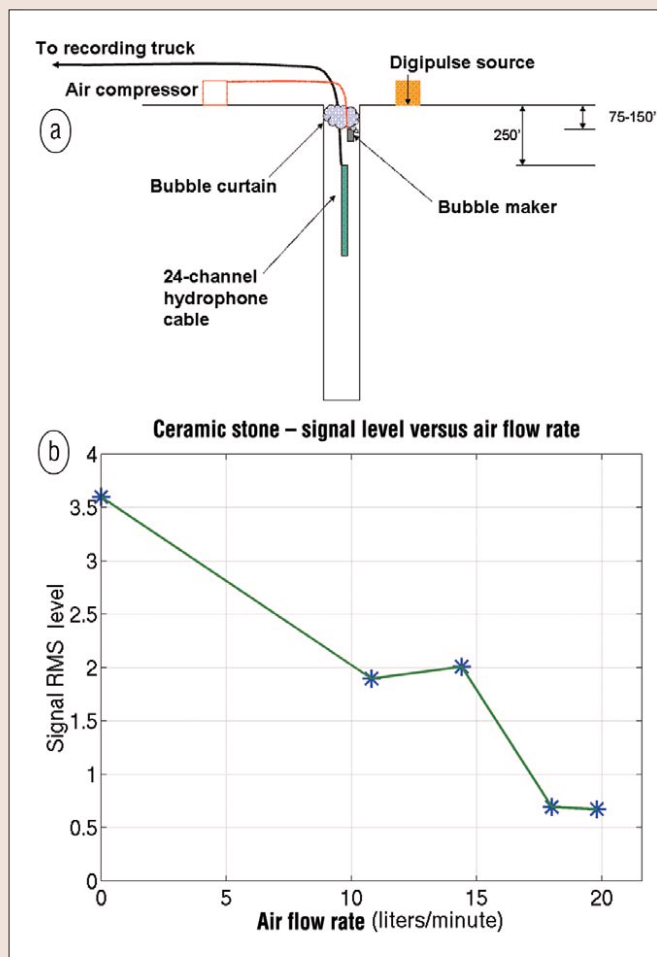


Figure 3. (a) Concept of tube-wave suppression via bubble curtains, and (b) tube-wave signal level as a function of air volume flow rate.

itive roots" in number theory (Schroeder, 1995), is optimally designed to minimize the backscattered energy (downgoing multiple) after reflection.

The bubble curtain created at the above-described plane remains in the water for some time after it is emitted. This latency in rising out of the water allows the curtain to take on a three-dimensional shape by extension in the inline direction (Figure 2c). The length of time the curtain remains in the water is, hence, a critical parameter in determining the size of the bubble curtain object as a multiple deflector. We discuss bubble-curtain latency and research into methods of controlling it in detail below.

Mitigating noise emanating from construction and facilities. The idea of protecting structures from waterborne noise by bub-

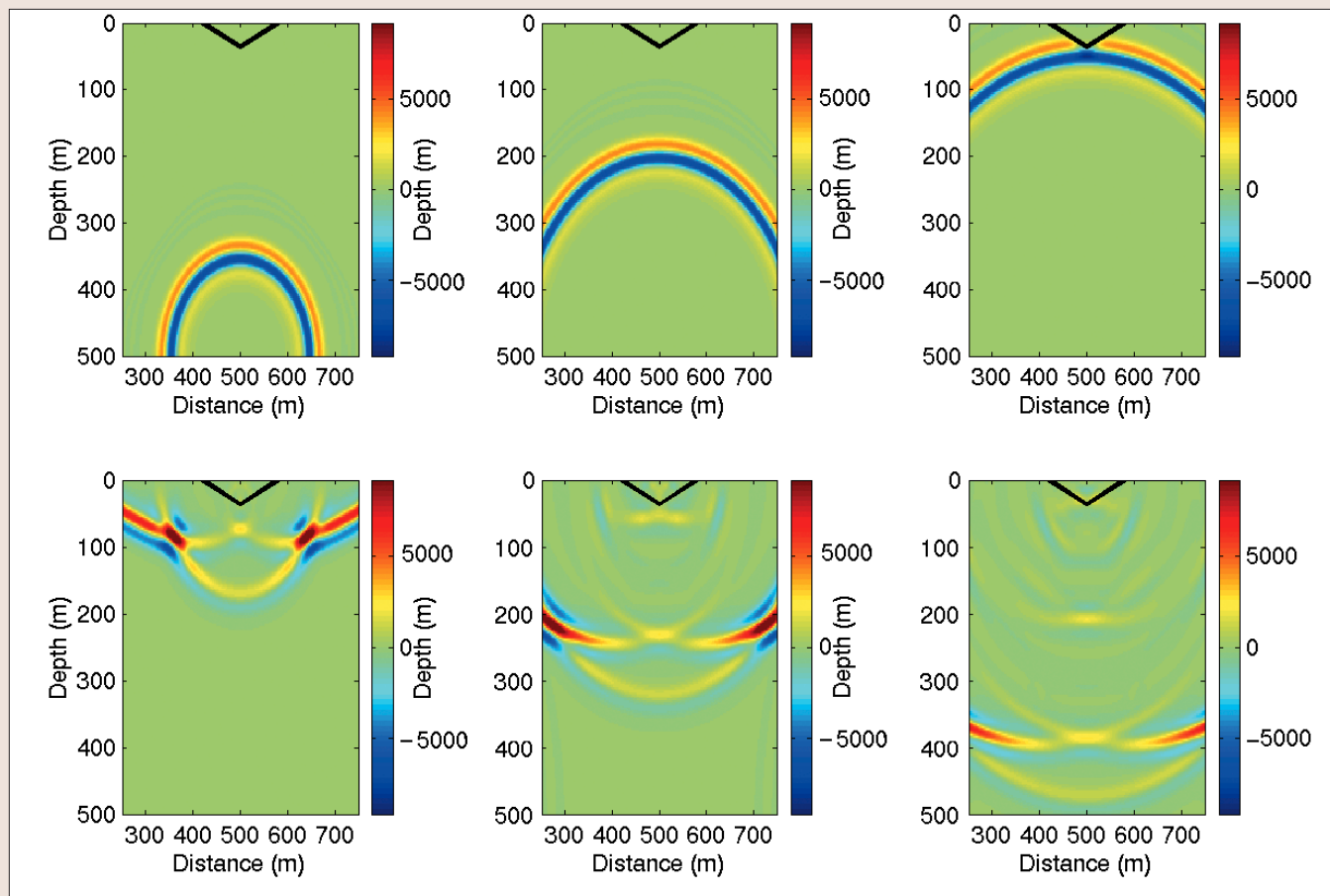


Figure 4. Snapshots of the wavefield as it propagates upward towards the air-water interface and interacts with the blanket.

ble curtains is not new. La Prairie patented the idea in 1955 as a means of protecting a dam from the damaging effects of explosions across a forebay, and saving the cost of draining the forebay. This idea has been implemented recently at the Hong Kong airport where a pile driver was surrounded by a bubble curtain to protect the nearby shoreline. Another current application is the ringing of piles with “bubble trees” at the San Francisco-Oakland Bay Bridge extension.

Potential applications are numerous in the petroleum industry. When noise from machinery on platforms, or from tankers, needs to be mitigated, solutions can be expensive (e.g., building permanent concrete berms or even changing the location of the noise-creating structure). Bubble curtains afford a relatively inexpensive solution and one that is portable in principle. Furthermore, offshore structures often have sufficient power and/or compressor capacity to easily accommodate the operation of bubble curtains.

Tube-wave suppression. Tube waves are an important noise in VSPs. In particular, for land VSPs, ground roll reaching the head of the well converts very effectively into tube waves and reverberates up and down the well. Over the years, several devices have achieved partial success in mitigating these noises.

A small amount of air injected in the top of the well achieves very high tube-wave suppression. One recent patent (Naville et al.) proposes creating mini-explosions in the well to supply such air. However, a small amount of compressed air directly injected in the top 50-100 m of the well may achieve a similar effect. By using this method, we have observed suppression ratios of a factor of six. Figure 3 shows the concept and a plot of tube-wave amplitude as a function of air volume flow.

Seismic interference. There are several types of noise labeled

seismic interference; some are amenable to a bubble curtain solution and others are not. What is commonly known as seismic interference noise occurs when two nearby vessels are shooting seismic data at the same time. If they do not agree to time share (which is very expensive), acoustic energy from shots emitted by one vessel can be recorded on the streamers (or bottom cables) of the other. This is very difficult to block because the noise source is moving in an unpredictable relationship to the recording array. It could be easier to avoid recording this noise if each shooting vessel could deploy a bubble curtain to block emanations from its own source. However, even in such a case, the receiving array of the other vessel may be in an unpredictable position and therefore the direction to block emanations would still be unknown.

The kind of interference noise that is most amenable to a bubble curtain solution occurs when the noise source is stationary or quasi-stationary—i.e., platforms or other facilities in the neighborhood of the seismic survey, noise created by vessels participating in the survey, or noise created by localizable marine life (e.g., shrimp). In one case we are aware of, noise created by the engines of a cable-laying vessel could easily be observed on the bottom cables of the active part of an OBC survey. Such noises are very noticeable on horizontal bottom phones. Because the cable-laying vessel is moving very slowly, the noise it creates could be blocked by a small bubble curtain deployed over the side of the vessel. This would be similar to the “masker” configuration used by the U.S. Navy to avoid detectable noises emanating from machinery aboard its vessels.

Multiple suppression. The acoustic blanket concept, for multiple suppression, is to create a highly reflective surface that will deflect an upcoming seismic wave before it reflects directly

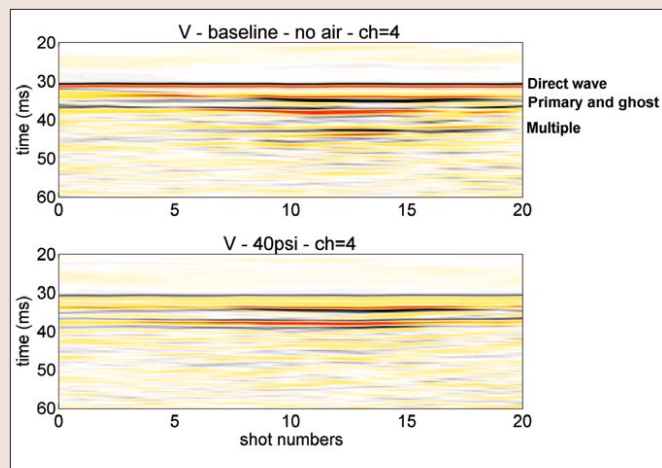


Figure 5. Images with (bottom) and without (top) the V-shaped grating. With the acoustic blanket, the multiple is suppressed. The direct wave is also suppressed because the bubble curtain is deployed in the direct path between source and receivers.

downward from the air-water interface. The shapes shown in Figure 2 are only two of a large class of such potential shapes. The primary characteristic of this class of shapes is that advantageous phase delays are introduced into the seismic wave that minimize downward reflection.

Whichever shape is chosen, one can obtain the far-field response of the array by computing its discrete Fourier trans-

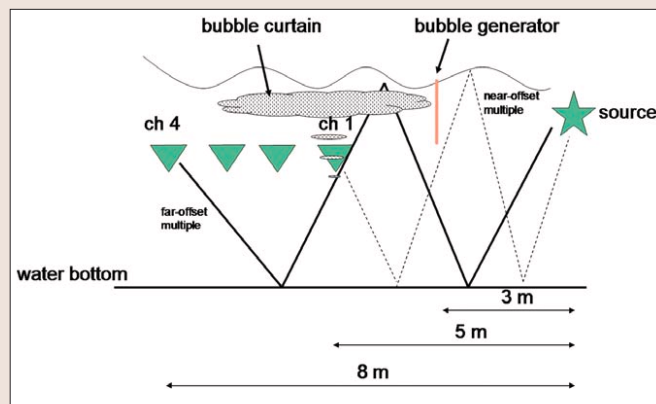


Figure 6. Ray diagram for the bubble curtain operation during small-scale seismic test.

form, and one can model the exact response of the array by acoustic simulation or other wave-equation modeling methods. Figure 4 shows snapshots from an acoustic simulation of the interaction of an upcoming wave with the V-shaped acoustic blanket. The blanket clearly puts a hole in the seismic wavefield, and redirects the highest concentration of energy at an angle to the vertical. The amplitude of the wavefield in the central portion has been reduced to 16-41% of its original value by the blanket.

Small-scale field tests. Small-scale field tests of the acoustic blanket concept were conducted at ExxonMobil's seismic test facility in Friendswood, Texas, U.S. in 2000. The Friendswood seismic pond is a 60×60 m body of fresh water with a maximum depth of 7 m. Both the V-shaped and primitive roots phase gratings were tested, although only the former is presented here. A miniaturized marine experiment was simulated by towing the bubble-making shapes, the source, and a four-channel hydrophone array along a single line with an electric winch. The seismic source was a 15 in^3 water gun that generated frequencies from 200 to 5000 Hz (filters applied in processing cut the upper end to 1100 Hz). The dimensions of the blankets were 8-12 m in the crossline direction and 2-4 m vertically. The blankets consisted of ceramic bubble-making stones affixed to a metal frame. Seismic data were collected and processed with this configuration, and multiple suppression measured by comparing the strength of the multiples with and without the blanket.

Figure 5 shows the images with and without the V-shaped grating. The image is shown for channel 4 (far offset, 8 m from the source). The events labeled in the baseline image are the direct wave, the primary water-bottom reflection and its ghost, and below that a strong multiple. Observe that the primary reflection and, hence, the multiples do not appear uniformly across the section but are high in amplitude toward the middle of the section. This middle section is the relatively flat deep portion of the pond. In this portion, pond geometry and strong bottom reflectivity (due to decaying organic matter settling at the bottom and outgassing) combine to give high reflectivity. By comparing the bottom and top images, we see that the bubble curtain is very effective at suppressing the multiple in the data. Measured suppression factor (SF) for the multiple is 2.5 in the center of the image, where the multiple is strong.

Figure 6, the ray diagram for the bubble curtain operation, shows that the bubble curtain does not cover that part of the air-water interface where the multiple recorded on channel 1 bounces. Consequently, we would not expect good multiple suppression on channel 1. This was supported by the results and highlights that the bubble curtain must be present at the bounce point of each multiple.

An important question is how an acoustic blanket com-

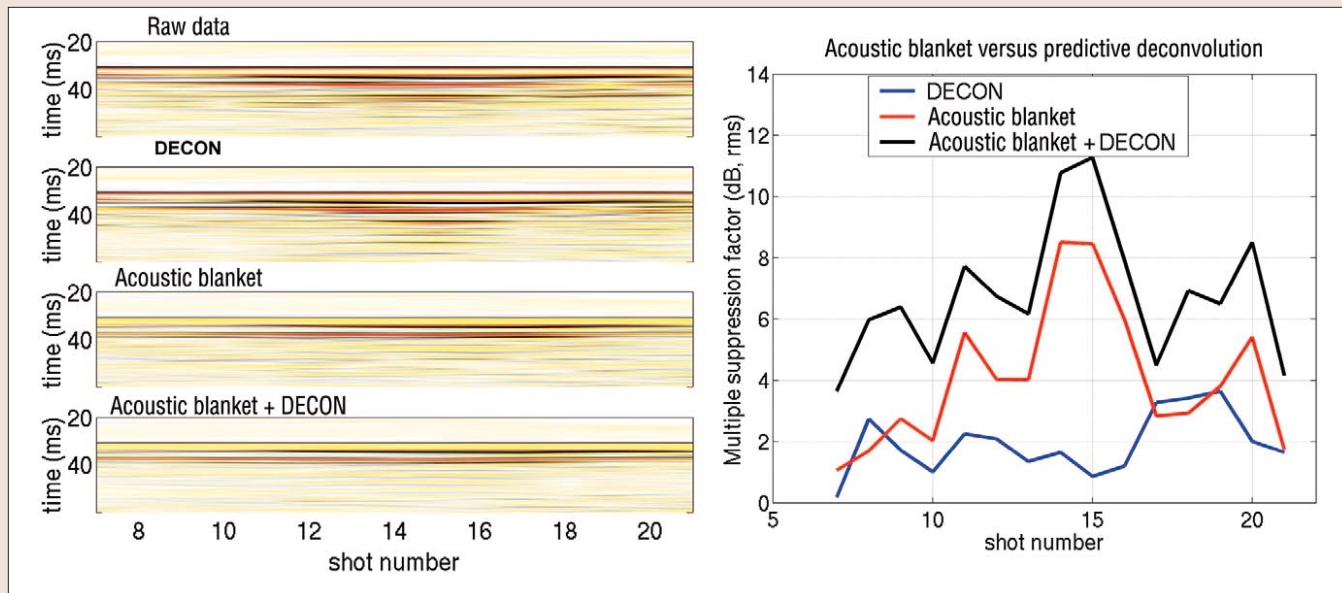


Figure 7. Comparison of the acoustic blanket results shown above to deconvolution.

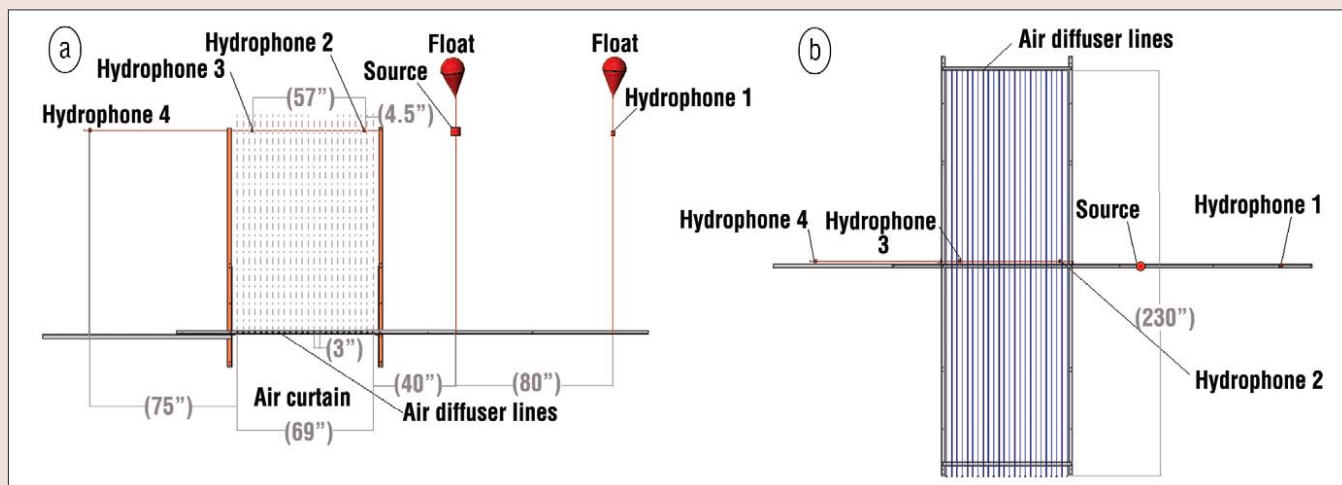


Figure 8. Setup for the stationary frame measurements: (a) side view, (b) plan view.

compares in multiple suppression to what can be achieved in processing. Figure 7 compares the acoustic blanket results shown above to deconvolution. (Because of a relatively small range and number of offsets, Radon filtering is not a viable option for multiple suppression in this example.) The figure compares predictive deconvolution applied on the raw data with bubble-curtain results for the V structure. Deconvolution barely reduces the multiple amplitude (only 2 dB suppression) and adds an artifact after the multiples, in the form of an additional reflection. This could be expected from the nature of the multiples in this dataset because the geometry of the pond causes the multiple train to be cut short (only one multiple following the primary). Predictive deconvolution, which is based on a mathematical model of a continuing series of multiples, performs poorly and creates an artifact after the last multiple when the multiple series is truncated. In this case, the bubble curtain does a much better job of suppressing multiples and achieves 8 dB suppression. The blanket, of course, makes no assumption about the mathematical character of the multiple series after generation. It relies on the physical fact that the multiple is generated by a wave turned around at the air-water interface, and blocks that generation mechanism. The figure also shows that any residual left by the acoustic blanket can be further reduced by applying deconvolution. This demonstrates the beneficial effects of combining acquisition-

and processing-based methods of multiple suppression.

In some model simulations, processing methods were more effective at reducing multiples than a simulated acoustic blanket. Thus, if we were restricted to one method alone, processing would be the better choice in those cases. However, in all our simulations, as in the field tests just cited, combining the two methods yields multiple suppression factors higher than either one alone. This conclusion may or may not generalize to the most sophisticated wave-equation multiple-elimination methods, but it is likely to apply generally for Radon filtering and deconvolution.

Offshore tests. To facilitate the design of an ocean-worthy acoustic blanket, several measurements of acoustic and mechanical properties of a prototype acoustic blanket were made during 10-16 January 2002, onboard the PGS vessel *Ocean Explorer*. We measured the reflection coefficient of a bubble curtain, the rise time of bubbles, the tow characteristics of a prototype structure, air-flow rates, and other variables relevant to an eventual implementation.

The bubble makers were rubber "weeping" hoses rather than ceramics used in the Friendswood tests (which were too fragile for offshore work). The hoses were a specially manufactured version of the weeping hoses available in home improvement stores. They emit bubbles a factor of 2-3 times smaller than those of the standard lawn variety, but larger than

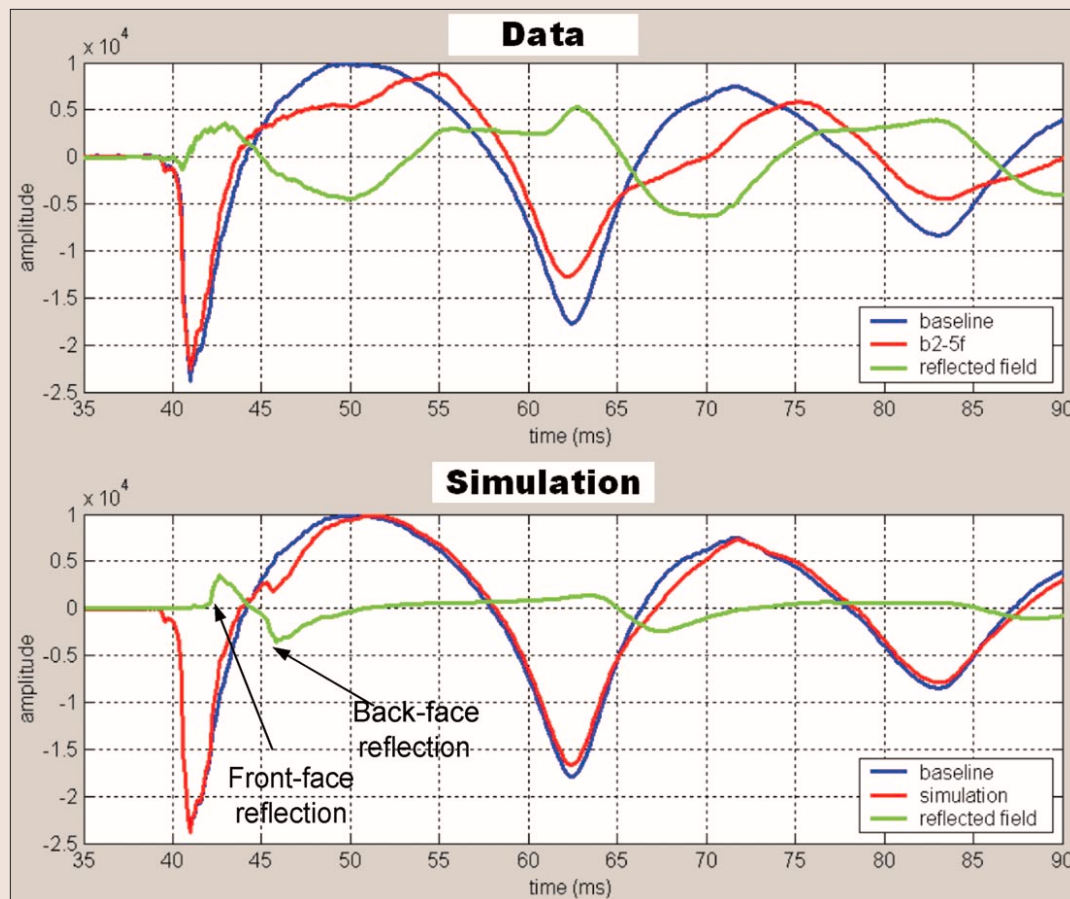


Figure 9. Baseline signal, the signal with the air curtain, and the reflected field, which is the difference between the two. (Top) Field data; (bottom) a full-wave simulation from a layered modeling program. The reflection from the front face of the curtain is the sharply rising edge of the reflected signal. The reflection from the back wall of the curtain immediately follows with opposite polarity within a few ms. The second large peak/trough combination at about 65 ms is a repeat of the front/back wall reflectivity combination when the bubble pulse hits the curtain.

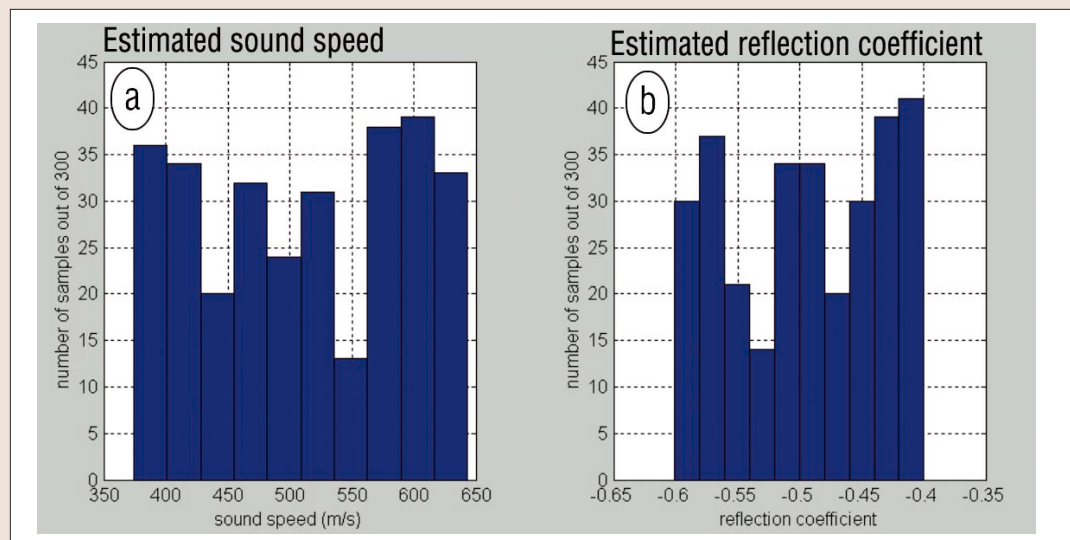


Figure 10. (a) Estimates of curtain velocity and (b) the implied far-field reflection coefficient of the curtain front face.

the bubbles produced by the ceramic stones.

The test was conducted offshore Gulf of Mexico in a water depth of 100 m. The test goals were divided into two parts—those that must be performed under tow and those requiring a stationary condition. All acoustic measurements were made using a stationary frame lowered to 25 m. As described below, bubble hoses were attached to an aluminum frame and acoustic measurements of both bubble rise time and bubble-curtain reflectivity were made approximately 3 m above the bubble-hose bed. In addition to the stationary test, a 10-m prototype of an acoustic blanket was towed at speeds up to 4.5 knots. Drag and stability characteristics of this prototype were observed, using pressure measurements and in-water video. Only the acoustic tests are presented here.

- **Experimental setup.** Figure 8 shows the setup for the stationary frame measurements. An aluminum frame, about 2×6 m, was threaded with 24 bubble hoses. The frame had vertical members 3 m above the hoses that support a crossbar from which hydrophones are deployed. The frame also had outrigger extensions that allow a source and other hydrophones to be deployed outside the bubble curtain. Four hydrophones were used, one 2 m behind the source, two inside the curtain, and one on the outside of the curtain attached to a far-side outrigger beam. The hydrophones were numbered 1-4 starting with the hydrophone behind the source.

Two sources were used for the experiment. A high-frequency piezoelectric crystal, driven at 10 kHz, was used for the rise-time measurements, where precision pin-

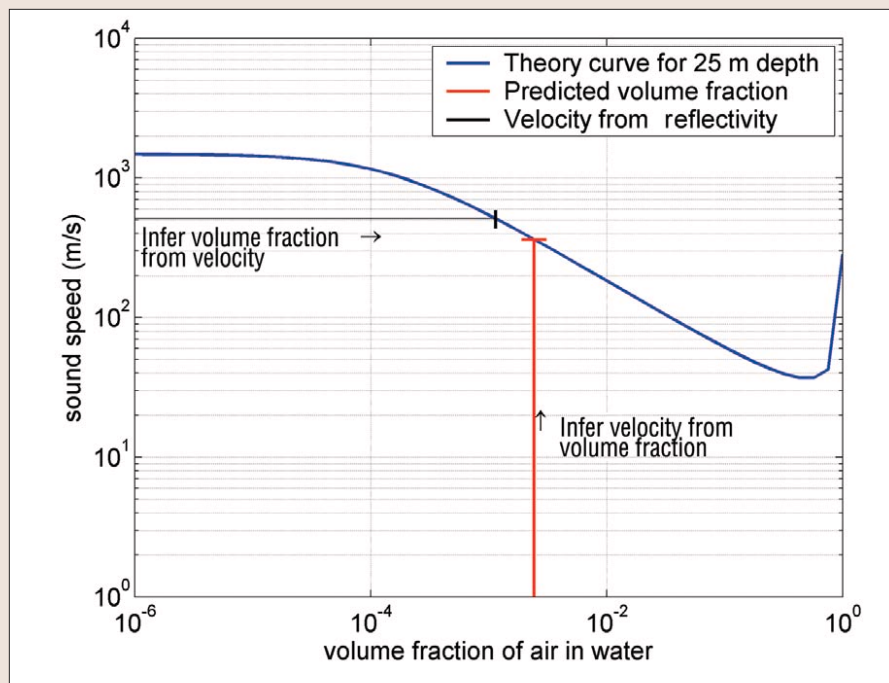


Figure 11. Sound velocity versus air volume fraction (Woods equation) for a depth of 25 m. In addition to the Woods equation theory curve, the figure shows the range of sound speeds estimated in the reflectivity analysis, projected onto the theory curve (black error bar). The figure also shows the range of volume fractions (red error bar) estimated from air volume flow measurements during data acquisition, projected onto the theory curve.

pointing of the curtain is necessary. An air gun with a 40 in³ chamber, pressured at 800 psi, was used for reflectivity measurements. Each source was placed at the location marked “source” in Figure 8, during the experiment.

The key instrumentation on the frame was a set of pressure transducers—several for the hoses, and two measuring the ambient pressure on each end of the stationary frame. The hose measurements allowed us to pressure the bubble hoses to the right level to obtain the needed flow rate. The ambient pressure measurements were used together as a level to confirm that the ends of the frame were close to the same depth in the water (within 2 ft) during the measurements. All pressure measurements were recorded continuously during data acquisition, as were the flow meter and acoustic data.

The frame was deployed over the side of the *Ocean Explorer* using two cranes to curtail rotation. Bubble curtain stationarity was critical in making the acoustic measurements successfully. Ship thrusters were used to obtain zero relative speed between the frame and ocean currents.

- **Bubble-curtain reflectivity.** An air gun was the source. Seismic data were collected at all hydrophones but data from the “back” hydrophone (1) is discussed here. Baseline measurements were made with no air-bubble curtain. Then, with air curtains of varying thickness, data were collected and compared with baseline measurements to determine reflectivity.

The dominant wavelength in the air-gun signature is 30 m. To minimize the diffraction around the air curtain, the source and hydrophones were placed very close to the curtain, approximately 1 and 3 m away, respectively, for the source and back hydrophone. This reduced diffraction significantly. However, it was still necessary to compute and compensate for the frequency-dependent diffraction around the curtain. Full-wave modeling matched to the data allowed estimation of the far-field acoustic reflection coefficient.

Figure 9 shows the baseline signal, the signal with the air curtain, and the reflected field (the difference between them). The top panel shows the field data and the bottom panel shows a full-wave simulation from a layered modeling program. The first part of the reflected field, arriving within 2 ms of the peak input signal, is the reflection from the front face of the curtain. After that, the reflection from the back wall of the curtain is visible as an opposite polarity peak. Observe that the model simulation shows this back wall reflection to be a sharp, well-defined peak, whereas in the measured data it is broader and less well defined. We also noted that this back-wall part of the signal is more variable from shot-to-shot than the first peak energy. This can be attributed to the fact that the signal is interacting with the interior of the bubble curtain, which is a fluctuating, inhomogeneous medium. Despite these differences between model and measured results, the general character is similar, and in particular the reflection amplitude of the first peak matches well. We confirmed with modeling that the amplitude of this first peak is unaffected

by the presence of the back wall of the curtain.

Figure 10 shows the estimates of curtain velocity and the implied far-field reflection coefficient of the curtain front face, based on comparing the amplitude of recorded data to a library of modeled responses with varying reflection coefficients. Three sets of measurements were used for these analyses—corresponding to curtain thicknesses of .84, 1.14, and 1.45 m. Taking all combinations of 10 baseline measurements with 30 reflected field measurements yields 300 independent estimates of the curtain velocity. The estimates range from 350 m/s to 640 m/s, and yield far-field reflection coefficients between -0.4 and -0.6. Velocity inside the curtain is estimated to be 512 ± 82 m/s. Curtain reflectivity is -0.49 ± 0.06 . Data transmitted through the bubble curtain to the far hydrophone (4, data not shown) confirm the curtain velocities estimated from the reflected data.

Figure 11 shows a plot of Woods equation (sound velocity versus air volume fraction) for a depth of 25 m. The figure also shows the range of sound speeds from Figure 10a, estimated in the reflectivity analysis discussed above. The volume fraction of air emitted during the test is superimposed. This volume fraction was computed from measured total air flow through the hoses during the experiment, taking into account the geometry and average rise rate of the bubbles. Both estimates, sound speed and air-volume fraction, fall on the same part of the curve. The reflectivity estimates of velocity are between 400 and 600 m/s. The volume-fraction estimates of velocity are somewhat lower, between 300 and 400 m/s. Despite these differences, integration of these two types of data confirms that air supplied in roughly the volumes we injected can lower the sound speed to a third of that in undisturbed water. This is an important confirmation of the theory underlying the acoustic blanket idea, and supports use of this theory to make design calculations for required air for other parts of the curve.

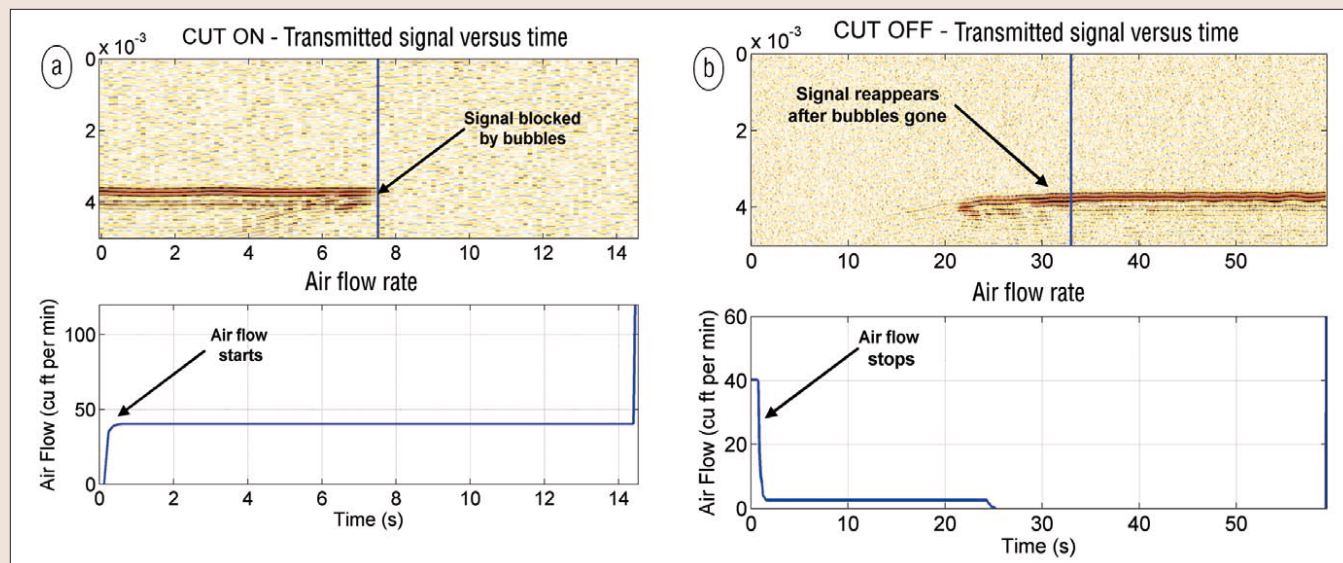


Figure 12. Two types of measurements: (a) "cut on," in which air is turned on and acoustic signal is blocked once the largest bubbles reach the transmission path, and (b) "cut off," in which the air is turned off and acoustic signal returns once the smallest bubbles have cleared the transmission path.

- **Bubble rise-time measurements.** During bubble rise-time measurements, the piezoelectric crystal source pinged repeatedly at approximately 0.1-s intervals. Reception was at all four hydrophones, but for the present discussion the data on the far hydrophone (4) will be used. A bubble curtain with a thickness of 1 m was generated for all rise-time measurements. In addition to acoustic signal, air flow was measured and recorded so that accurate on and off times of the curtain could be determined.

Two types of measurements were made to determine the rise rates of the largest and smallest bubbles respectively. They are denoted by "cut on" and "cut off" in Figure 12. In the cut-on measurement, the air flow was started and data were recorded until well past the time when no signal appeared on the hydrophone. At this point, the largest bubbles have reached the level of the source-hydrophone, and they block reception of acoustic signal. In the cut-off measurement, the air flow was on in steady state, and was then stopped. Data were recorded until well past the time when signal reappeared on the hydrophone. At this point, the smallest bubbles have passed the source/hydrophone level and no longer block reception of acoustic signal.

The cut-on times were well demarcated with little ambiguity. The cut-off times, on the other hand, are harder to pick and subject to more interpretation. We chose the point at which signal fully reappears. This picking strategy gives times consistent with video observations of bubble size in the lab.

Figure 13 composites the rise rates for several repeat measurements, based on the observed times and the vertical distance of 2.3 m from bubble hose bed to the level of the hydrophones. The rise rate for the smallest bubbles ranges from 6.0 to 9.4 cm/s, and for the largest

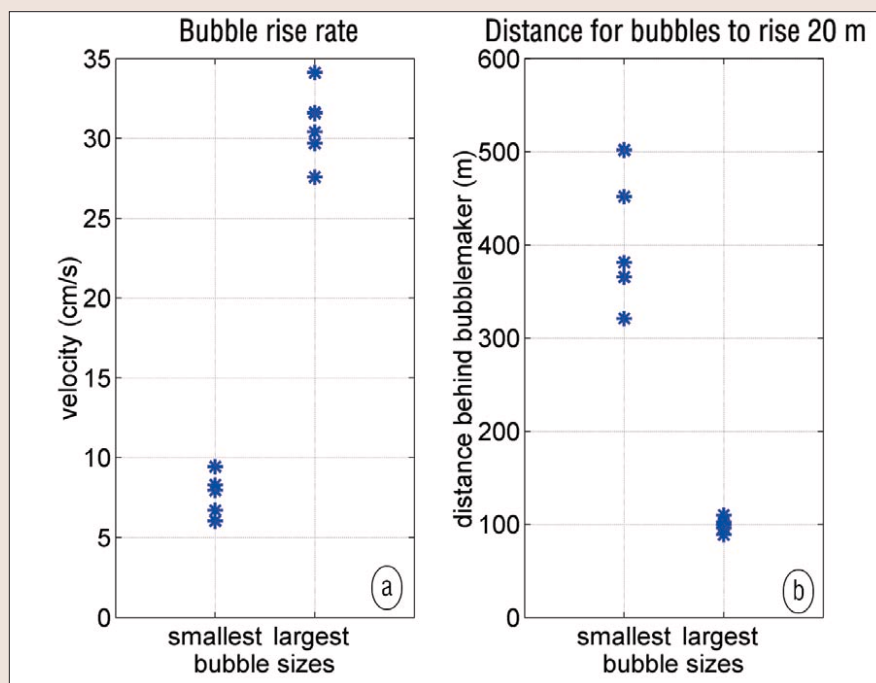


Figure 13. (a) Rise rates, (b) distance bubble curtain will remain behind the bubblemakers under the normal seismic vessel speed of 4 knots.

bubbles it ranges from 27.6 to 34.1 cm/s. Figure 13b translates these rise rates into distance the bubble curtain will remain behind the bubble makers under the normal seismic vessel speed of 4 knots. For this calculation, it is assumed that the bubble curtain is formed at a depth of 20 m, and that it rises with an average velocity to the surface 32% faster than the measured velocity. This increase in the rise rate accounts for the acceleration of bubbles as they rise toward the surface (Vermillion, 1975). The largest bubbles will have risen 20 m at a distance 90-110 m behind the bubble maker. The smallest bubbles will have risen 20 m at a distance 320-500 m behind the bubble maker.

These predictions of curtain extent highlight one key technical issue in implementing bubble-curtain multiple suppression. These extents do not cover enough of the streamer to suppress the receiver-side as well as the

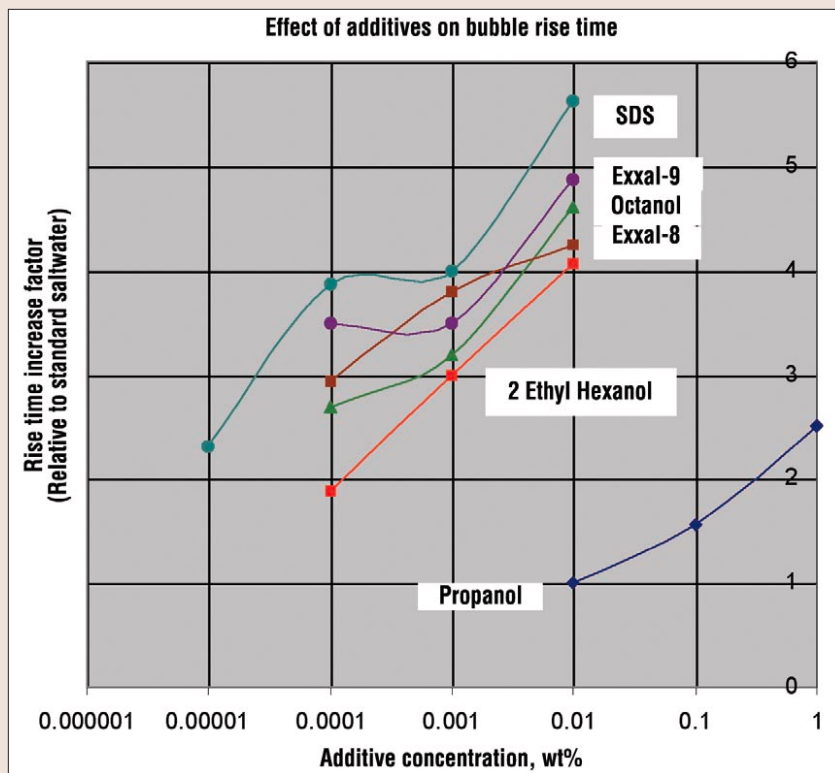


Figure 14. Increase in bubble longevity in seawater with small amounts of several additives.

source-side multiples. To fully reach their potential, bubble curtains must cover 3000-5000 m of the streamer.

Practical implementation issues. Extending the length of the curtain is discussed in detail in the next section. Several other implementation issues not addressed in this paper must also be considered in order to make the acoustic blanket practical. Among them are the effect of ocean currents, integration of a bubble curtain into streamer operations, required air volume, and cost. Ocean currents move the bubble curtain, since bubbles move when the water moves. This is a major problem when the bubble curtain remains a long time in the water because currents can move the curtain a long way. As an example, a 1 knot current will move a bubble stream 60 m in two minutes. Bubble curtain size and deployment must take such movement into account. High currents, and especially crosscurrents that vary with depth, might deteriorate the effectiveness of a bubble curtain to the point that it would be unusable.

To block the downward reflection from the air-water interface without interfering with the primary reflection, the bubble curtain must be deployed *above* the seismic streamer. Thus, the streamer must be lowered to more than 30 m. The bubble curtain must be deployed near the source, close enough that the bubble curtain sufficiently surrounds the bounce point of the near-offset multiples. Otherwise, it will not suppress them effectively. The towing and careful positioning of a frame that requires large air volumes and hoses, supplied from onboard compressors or additional air-supply vessels outboard of the seismic spread, add complexity and safety issues to the implementation.

Note that a 30-m streamer depth does not imply a low-frequency first ghost notch, as might first be assumed, because the curtain reflecting interface is only a few meters above tow depth. There may be receiver ghost issues, however, as the curtain changes its depth with distance along the streamer, ultimately disappearing from the water. Processing solutions

(such as dip filtering or ghost deconvolution) must be developed or tailored to handle an offset-dependent ghost variation.

Required air volume flow rate is a function of the blanket dimensions, volume fraction of air in water, vessel speed and percentage of "useful" bubbles (bubbles that do not rise out of the system too quickly). A 350-m blanket injecting a 2-m thick curtain with a volume fraction of 0.002 into seawater, towed at a speed of 2 m/s (4 knots), requires 18 000 standard ft³ per minute (scfm) if all the bubbles are useful (a perfectly efficient system). If only 25% of the bubbles meet that standard, 72 000 scfm are required. These air volumes are very high by seismic standards: A seismic vessel might have two 1500 scfm compressors onboard. However, it should be noted that the air pressures required for an acoustic blanket are only incrementally above ambient pressure at depth (enough to pressure bubble makers above head pressure). For a given air-handling capacity, cost and complexity of low-pressure compressors are significantly lower than for the high-pressure compressors used with air-gun arrays.

Nonetheless, air compressors and the fuel to run them dominate the cost of an acoustic blanket system, and system efficiency is a critical cost determinant. Cost of a system that would cover a multistreamer 3D survey represents a 37% premium over daily 3D survey costs. Of this, 80% is attributable to compressors. To be sure, these are research costs and would be subject to lowering with economies of scale and improvements in the technology. Furthermore, multiples are so severe a problem in some areas that significant acquisition cost increments have been incurred to address them.

Preliminary bubble-size reduction experiments. As is clear from the above predictions of curtain length, longevity of bubbles in the water is an important unsolved challenge. In the offshore test, rise rates for the smallest bubbles were measured to be about 6.0-9.4 cm/s, which yields a bubble curtain that covers approximately the first 400 m of the streamer. Modeling shows that the bubble curtain must have an extent in the inline direction of at least a kilometer to meet minimal multiple-suppression requirements, even for the source-side multiples. Preferably, the bubble curtain would extend over a substantial portion of a seismic streamer, in order to suppress receiver-side multiples as well.

Meeting this technology hurdle requires the improvement of bubble-making hoses to emit bubbles with mean radii of 50-75 microns, a factor 2-3 smaller than currently available. In addition to extending the coverage of the bubble curtain, this reduction of the bubble size has important efficiency implications: One bubble with a radius of 150 microns contains nine times the air volume of a bubble with a radius of 50 microns. This air volume is wasted, as large bubbles rise out of the water too rapidly to be of practical use.

Research on hose improvement, in collaboration with ExxonMobil Corporate Strategic Research labs in Clinton, New Jersey, USA has identified several promising chemical additives that inhibit bubble coalescence and promote bubble detachment at a small size. Most of these additives are alcohols of differing carbon-chain lengths. Figure 14 demonstrates the increased longevity of bubbles in seawater containing small percentages of several additives. A 0.01 weight % of

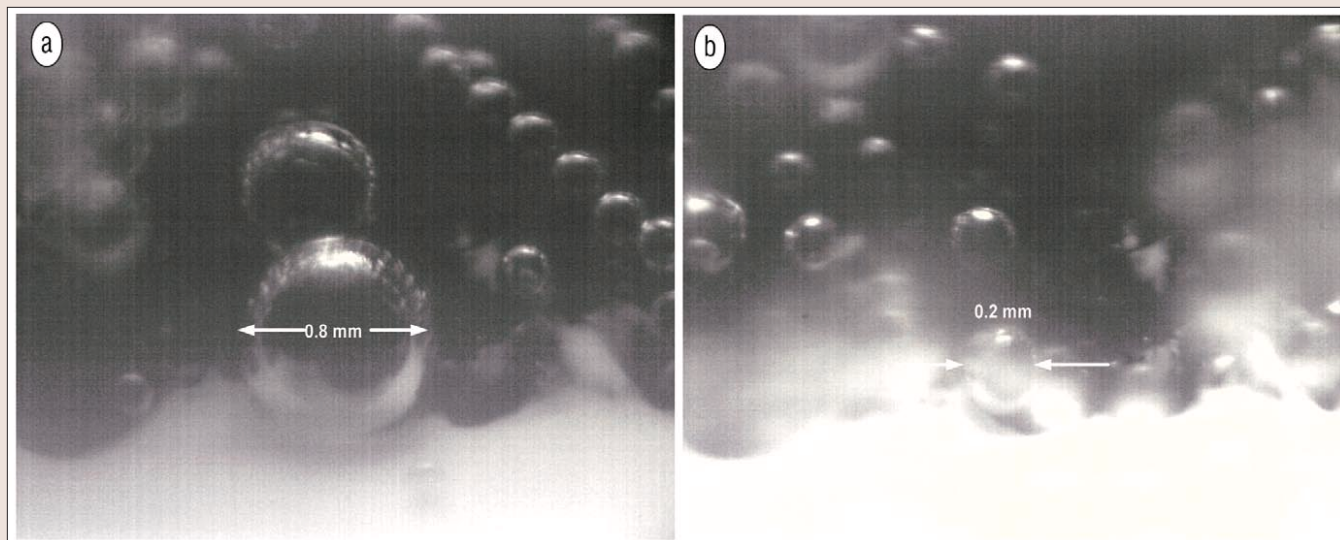


Figure 15. Bubble emitted from a single pore. (a) Bubble in stationary water is 0.8 mm in diameter. (b) Bubble in water moving at 2 m/s is 0.2 mm in diameter.

octanol, for example, increases the time required for bubbles to reach the surface by a factor of 4.5. Other alcohols of different chain lengths are also effective, and effectiveness increases with chain length. Surfactants such as sodium dodecyl sulfate (SDS in Figure 14) are also very effective. The key to using these additives is delivery. Several methods of application have been tested, including surface coating of the bubble-making hoses and suspension of the additives in the air mixture, diffusing them with the air through the hose pores. Results of the coating method to date only show short-term improvement before the additives wear off or are dispersed. The suspension approach has also been ineffective thus far, due to inability to supply large enough volumes of the additive without condensation and clogging. Methods need to be developed to more permanently affix these additives to the hoses, incorporate them in the hoses, or force them through the pores without condensation.

A recent test of another method to reduce bubble size relies on the flow of water across the bubble-making hose surface, which naturally occurs as the hoses are pulled through the water. The test showed substantial reduction of the largest bubbles. Figures 15 and 16 show that bubbles that are normally emitted at a radius of 300–400 microns are reduced in size to 100–200 microns by water flow. The smaller bubbles, however, are not reduced by the crossflow of water, which is demonstrated in the figure by both the constant size of the smallest bubbles and by the limitation in the reduction of the larger bubbles. The limitation results from a quiescent boundary layer near the surface of the hose where water flow speed is very small (approaching zero at the hose surface—the so-called “no slip” condition in fluid dynamics). These smaller bubbles represent the vast majority of those created by the bubble hoses, and are the ones responsible for the bubble curtain’s longevity in the water after bubble emission. They must be reduced further in size if the bubble curtain is to last long enough in the water to cover most of the seismic streamer. Based on observations from these

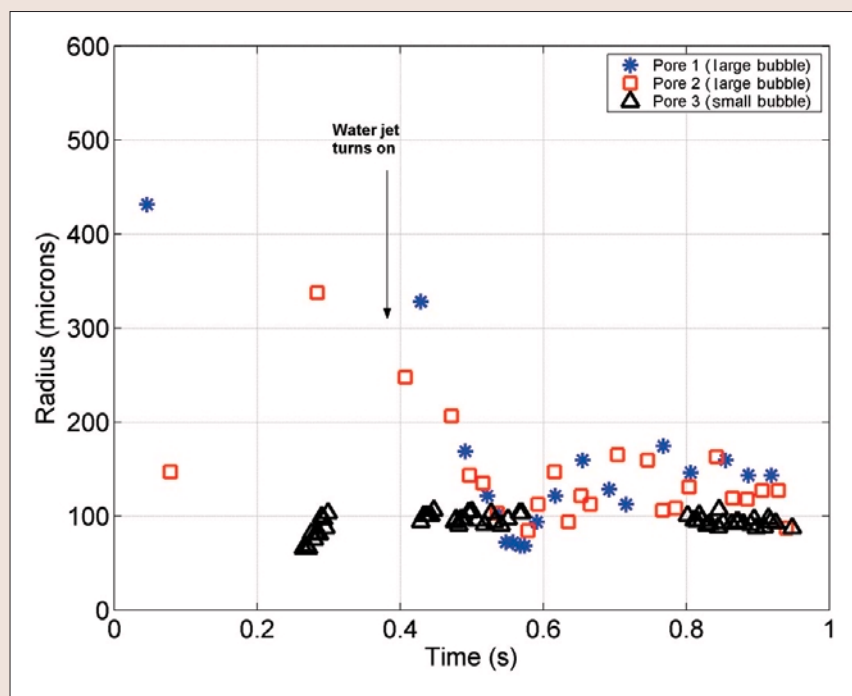


Figure 16. Radii of bubbles tracked over time as they emerge from three nearby pores. Radii of large bubbles from two pores are reduced from 300–400 microns to 100–200 microns with moving water. Radii of smaller bubbles from third pore are unchanged with moving water.

tests, several possible physical improvements to the hose design have been identified that would enable the crossflow effect to reduce bubble size for all bubble diameters. The improvements all rely in physical configurations of bubble-making hoses that interfere with the development of a boundary layer, such as reducing long runs of straight hose. These ideas remain to be tested.

Conclusions. Bubble curtains are effective at mitigating a wide range of underwater noises in both seismic and non-seismic contexts. The research on bubble curtains began with the moving bubble-curtain application (multiple suppression) because of the importance of multiple suppression to improved seismic data quality. The method has been demonstrated on a small scale at the ExxonMobil seismic test pond, where multiple suppression of 8 dB was demonstrated for the bubble

curtain alone, and an additional 2 dB was obtained by applying deconvolution on the data recorded with a bubble curtain. Basic data for the design of bubble curtain multiple suppression have been obtained in an offshore test with Petroleum Geo-Services. This test established the high reflectivity of a bubble curtain at seismic frequencies. The test also confirmed the Woods equation relationship between air volume fraction in seawater and acoustic sound speed in the bubbly mixture, at a point on the curve close to the design operating point.

The method presents several implementation challenges, the most important being the longevity of the emitted bubbles. For this reason, we have conducted initial research on methods of increasing bubble residence time in the water. At present, this work has developed promising leads, including the identification of additives that increase bubble lifetime and the quantification of the degree to which moving water itself extends bubble residence time. Several challenges remain. For the additives approach, delivery is the key issue. A method must be developed to deliver the additives without them wearing off too soon. For the moving water approach, a method must be developed to interfere with the quiescent boundary layer near the surface of the bubble-making hoses, in order for the moving water to shear the bubbles off with radii in the 50-75 micron range.

Despite these implementation challenges, there is much potential in such an acquisition-related method of removing multiples. We have shown that a combination of acquisition and processing methods is the most effective means of suppressing the most troublesome noises. The value of bubble curtains is further supported by the fact that several new applications have emerged in which bubble curtains are eas-

ier to implement because they are deployed in a stationary or quasi-stationary way. Six-fold suppression of tube-waves in boreholes has been demonstrated with a bubble curtain at the top of a well. We have also modeled and envisioned several uses for a shield that blocks noises emanating from vessel thrusters or other offshore sources.

Suggested reading. Tuned Bubble Attenuator for Towed Seismic Array by Behrens (U.S. Patent 5 959 938, 1999). Acoustic Lens for Marine Seismic Data Multiple Reflection Noise Reduction by Clark (U.S. Patent 4 625 302). "Acoustic wave propagation in air-bubble curtains in water—Part I: History and theory" by Domenico (*GEOPHYSICS*, 1982). Method of Blasting by La Prairie (U.S. Patent 2 699 117, 1955). Method for Multiple Suppression Based on Phase Arrays by Lee et al. (U.S. Patent 6 606 278, 2003). Seismic Prospecting Method and Device in Wells Allowing Guided Waves Filtering by Naville et al. (U.S. Patent 6 332 507, 2001). "Phase gratings with suppressed specular reflection" by Schroeder (*Acoustica*, 1995). "A look at some rising bubbles" by Vermillion (*American Journal of Physics*, 1975). "Development of an air bubble curtain to reduce underwater noise of percussive piling" by Wursig et al. (*Marine Environmental Research*, 2000). **TJE**

Acknowledgments: We acknowledge contributions in this work from Mike Norris, Phil Summerfield, Gary Szurek, Marv Johnson, Tom Murray, Robert Raschke, and Raymond Young (ExxonMobil Upstream Research Company); Chuck Morgan, John Krylowski, Bill Lamberti, Mike Pluchinsky, and Eric Sirota (ExxonMobil Research and Engineering Company); the crew of the Ocean Explorer; and Bill Pramik (Petroleum Geo-Services).

Corresponding author: warren.s.ross@exxonmobil.com